PHYSICAL REVIEW D **95,** 084049 (2017)

Testing gravity with pulsar scintillation measurements

Huan Yang,[1,2] Atsushi Nishizawa,[3,4] and Ue-Li Pen[1,5,6,7]

[1]*Perimeter Institute for Theoretical Physics, Waterloo, Ontario N2L2Y5, Canada*
[2]*Institute for Quantum Computing, University of Waterloo, Waterloo, Ontario N2L3G1, Canada*
[3]*Department of Physics and Astronomy, The University of Mississippi, University, Mississippi 38677, USA*
[4]*Theoretical Astrophysics 350-17, California Institute of Technology, Pasadena, California 91125, USA*
[5]*Canadian Institute for Theoretical Astrophysics, 60 St. George Street, Toronto, Ontario M5S3H8, Canada*
[6]*CIFAR Program in Gravitation and Cosmology, Canadian Institute for Advanced Research, 180 Dundas Street West, Toronto, Ontario M5G 1Z8, Canada*
[7]*Dunlap Institute for Astronomy & Astrophysics, University of Toronto, AB 120-50 St. George Street, Toronto, Ontario M5S 3H4, Canada*

(Received 9 July 2016; published 26 April 2017)

We propose to use pulsar scintillation measurements to test predictions of alternative theories of gravity. Compared to single-path pulsar timing measurements, the scintillation measurements can achieve an accuracy of one part in a thousand within one wave period, which means picosecond scale resolution in time, due to the effect of multipath interference. Previous scintillation measurements of PSR B0834 + 06 have hours of data acquisition, making this approach sensitive to mHz gravitational waves. Therefore it has unique advantages in measuring the effect of gravity or other mechanisms on light propagation. We illustrate its application in constraining the scalar gravitational-wave background, in which case the sensitivities can be greatly improved with respect to previous limits. We expect much broader applications in testing gravity with existing and future pulsar scintillation observations.

DOI: 10.1103/PhysRevD.95.084049

I. INTRODUCTION

Pulsar scintillation happens when pulsed radio signals from pulsars follow different paths of propagation to reach the Earth, and exists for almost all known pulsars. It is generally known that structures in interstellar plasma along the propagation path play the role of an effective "lens" and generate necessary lensing for pulses along different paths to meet at the Earth. Upon arrival, these radio signals interfere with each other and generate a spatially and frequency-varying interference pattern. As the Earth moves, an observer experiences time-dependent intensity variation corresponding to different fringes in the interference pattern. The nature of these lenses is not fully understood, but they appear to be dominated by rare, isolated coherent plasma structures. Quantitative models have been proposed to provide precision templates using a small number of optical caustic parameters [1,2].

As illustrated in Fig. 1, the spatial separation between fringes is approximately λ_e/α (λ_e is the radio wavelength, and α is the path opening angle) and the temporal separation is $\sim\lambda_e/(\alpha V_e)$, where V_e is the projected Earth-lens-pulsar velocity, generally dominated by the pulsar proper velocity. With α assumed to be ∼arcsec, one typically observes a scintillation time scale of seconds, typically longer than the pulsar period. By statistically (see the discussion in the next section) averaging over the time shift of the fringes, it is possible to achieve a phase accuracy that is equivalent to picosecond resolution in time. This is a factor of 10^5 higher than the accuracy in single-path pulsar timing [3]. It is worth noting, however, that scintillation measurements are fundamentally different from traditional pulsar timing measurements, where the relevant physical quantity in the former scenario is the radio wave phase

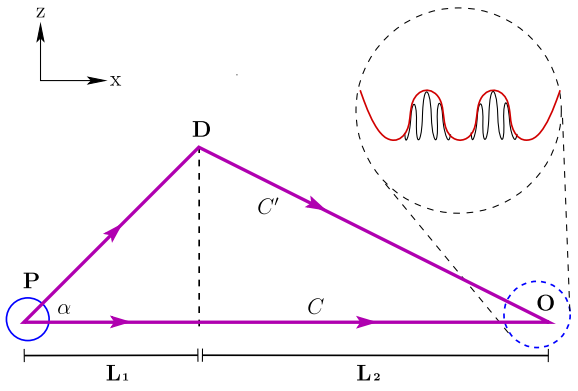

FIG. 1. The illustration for pulsed signals that arrive at the Earth following two distinctive paths, where the wave following C' is deflected by the interstellar medium at location "D." Here $L_1 = r/(1+r)L$ and $L_2 = L/(1+r)$. When the radio waves from these two directions reach the observer at the Earth, they interfere and produce a very fine interference pattern based on the radio wavelength λ_e and the path opening angle α. As the Earth moves at a speed $V_e \sim 30$ km/s, there are many fringes within the time scale of a single pulse (for illustration purposes we only show a few fringes within each pulse).

difference, and in the latter case it is the pulse arrival time. Therefore it is important to bear in mind that the "timing precision" in this paper actually refers to the phase accuracies in the phase.

This unprecedented phase accuracy (and equivalent timing precision) allows one to use the scintillation to probe the physics of plasma structures in an interstellar medium [4,5] and constrain the size of emission regions in the pulsar magnetospheres [6]. Although high-precision pulsar timing has been discussed extensively in the literature to test alternative theories of gravity, little is known about using scintillation measurements to test gravity. In this paper, we propose to use pulsar scintillation measurements as a laboratory for gravitational physics, in particular, as a detector of scalar gravitational waves (GWs), which appear in alternative theories of gravity. A similar analysis can be applied to test other physical effects that affect the propagation of radio waves.

A. Scintillation modulation

Propagating gravitational distortions modulate the plasma lensing effects. The plasma lenses can change shape on the sound-crossing time scale, which is typically 4 orders of magnitude longer than the gravitational time scales. This allows precise measurements of spacetime variations that are unlikely to be mimicked by plasma effects. If there exists a GW large enough to be detected, it would lead to an irreducible scintillation model residual.

In the absence of GWs, the variation of the plasma propagation Green's function is dominated by the Earth-lens-pulsar relative motion. Interstellar holography retrieves the time-dependent Green's functions, and has been demonstrated to reproduce observed scintillation patterns to a few parts per million [7]. The authors of Ref. [7] were able to decompose the dynamic spectrum as a sum of the kernels of Green's functions lying approximately on a parabolic set of loci. These lenses are located at a distance of 389 pc from Earth, with a pulsar distance of 640 pc [2]. The parabolic relationship arises from the collinearity of lensing points: the time delay through the lens is proportional to the square of its transverse separation angle. The doppler frequency is the time derivative of this delay due to the pulsar's apparent motion relative to the screen, and is linear in transverse separation, thus resulting in a parabolic relationship of the delay and doppler rate of the lensing images. As a result, plasma lensing induces a modulation frequency proportional to the image separation, whereas the change induced by GWs is independent of the separation. Such a pattern is not observed. We interpret the achieved dynamic range of 63 dB as implying that no modulation of more than a part in a thousand in the dynamic spectrum can be due to gravitational waves moving at the speed of light. The observing frequency was approximately 300 MHz, corresponding to a wave period ~3 ns and a Nyquist voltage sampling rate of 1.5 ns. We thus estimate the maximum contribution of gravitational waves as at most a part per thousand, or about a picosecond as the limit on the allowed inverse delay-doppler power. The lower bound of the measurable frequency is constrained by the total observation time $t_{\rm obs}$ (for the work in Ref. [7], $1/t_{\rm obs} \sim$ m Hz). The upper bound of the frequency is related to the separation between pulses $1/t_{\rm sep}$, as the pulse sequence determines a natural sampling frequency. A more precise analysis would require access to the data and holography algorithm.

The accuracy of this model is limited only by thermal noise, and not by pulsar self-noise. A typical $\Delta t \sim$ hour long observation with $\Delta\nu \sim 100$ MHz bandwidth leads to a flux uncertainty of SEFD$/\sqrt{\Delta t \delta\nu}$, where SEFD is the system equivalent flux density. For large telescopes such as FAST or Arecibo, SEFD is about 5 Jy. There are further subtleties which could affect the sensitivity of scintillation measurements for gravitational waves. First, the 63 dB in power or factor of 10^3 in signal-to-noise ratio (SNR) is achieved mainly near the bottom of the parabola in the decay time-doppler shift curve, where the signal is the strongest and the effect of GW vanishes. At larger opening angles the data could encode information about the GWs but the SNR is lower. Therefore for each specific data set one should try to find the optimum opening delay that balances these two effects. Second, it is possible that following the treatment in Ref. [7], part of the noise is absorbed in the model. Therefore it is unclear what fraction of the GW power remains in the residuals. Such a fraction may also vary depending on the types of GWs: i.e., single source, continuous/burst sources, GW background, etc.

II. PROBING NONTENSORIAL COMPONENTS OF GWs

According to the theory of general relativity (GR), GWs have only two tensor polarizations that are transverse to the wave propagation direction. However, in the general metric theory of gravitation [8], since the metric perturbation $h_{\mu\nu}$ has ten components, four of which are purely gauge and eliminated by imposing the condition $h_{0\mu} = 0$, there are six degrees of freedom left in h_{ij} $(1 \le i,\ j \le 3)$. Therefore gravitational wave emissions with scalar and vector polarizations are predicted in many alternative theories of gravity, such as scalar-tensor theory, $f(R)$ theory, bimetric theory, etc. (For a summary of GW polarization predictions in various alternative gravity models, see Ref. [9] and reference therein.) Measuring and/or constraining GWs with nontensorial polarizations are a viable approach to test the theories of gravity and search for possible new physics.

We follow the convention in Refs. [9,10] to label these six polarizations (two tensor modes: $+$ and $\times$; two vector modes: x and y; and two scalar modes: b, l). In the case that the GW is propagating along the z axis, the tensor bases are

$$\tilde{e}^{+}=\begin{pmatrix}1&0&0\\0&-1&0\\0&0&0\end{pmatrix},\quad \tilde{e}^{\times}=\begin{pmatrix}0&1&0\\1&0&0\\0&0&0\end{pmatrix},$$
$$\tilde{e}^{b}=\begin{pmatrix}1&0&0\\0&1&0\\0&0&0\end{pmatrix},\quad \tilde{e}^{l}=\begin{pmatrix}0&0&0\\0&0&0\\0&0&1\end{pmatrix},$$
$$\tilde{e}^{x}=\begin{pmatrix}0&0&1\\0&0&0\\1&0&0\end{pmatrix},\quad \tilde{e}^{y}=\begin{pmatrix}0&0&0\\0&0&1\\0&1&0\end{pmatrix}, \tag{1}$$

so that h_{ij} can be decomposed as

$$h_{ij}=\sum_{A}h_A\tilde{e}^{A}_{ij}. \tag{2}$$

As an illustration of applications of pulsar scintillation observations to testing gravity, we show that the existing data provide the best constraint on scalar gravitational wave background (GWB) in the mHz band, which beats the previous constraint by 4 orders of magnitude and might be improved by future space-based GW missions such as eLISA [11].

As shown in Fig. 1, we consider a train of radio waves emitted from a pulsar ("P") that propagates along two different paths ($\mathcal{C}$ and $\mathcal{C}'$) and eventually reaches the Earth. For simplicity, we consider only a one-time deflection by the turbulent plasma at location "D" (which is straightforward to generalize to cases with multiple deflections), and assume both paths are in the x-z plane, with $\mathcal{C}$ being along the x axis. The coordinates of "P," "D," and "O" in the x-z plane are $[0,0]$, $[Lr/(1+r), L r\alpha/(1+r)]$, $[L,0]$ respectively, where $r\equiv L_1/L_2$ in Fig. 1.

In order to obtain the sensitivity curve to GWs, we derive the transfer functions from GWs with frequency ω_g in such a system. Based on the standard pulsar timing analysis, the GW-induced phase shift of radio waves propagating along $\mathcal{C}$ is (hereafter we adopt the geometric units where the speed of light $c=1$)

$$H_C=\frac{\pi n^i h_{ij} n^j}{\omega_g\lambda_e}\frac{\sin[\omega_g L\xi+\psi]-\sin\psi}{\xi}, \tag{3}$$

where ψ is the initial phase of that particular GW, and $\xi\equiv 1-\mathbf{k}\cdot\mathbf{n}$, with $\mathbf{k}$ being the unit direction vector of the GW and $\mathbf{n}=\mathbf{e}_x$ being the unit direction vector of $P\to O$.

Following the same principle, the phase shift (due to the same GW train) of radio waves propagating along $\mathcal{C}'$ is

$$H_{\mathcal{C}'}=\frac{\pi n_1^i h_{ij} n_1^j}{\omega_g\lambda_e}\frac{\sin[\omega_g rL\xi_1+\psi]-\sin\psi}{\xi_1}+\frac{\pi n_2^i h_{ij} n_2^j}{\omega_g\lambda_e}\frac{\sin[\omega_g L\xi+\psi]-\sin[\omega_g rL\xi_1+\psi]}{\xi_2}, \tag{4}$$

where $\mathbf{n}_1=\mathbf{e}_x+\alpha\mathbf{e}_z$, $\mathbf{n}_2=\mathbf{e}_x-r\alpha\mathbf{e}_z$ and $\xi_{1,2}=1-\mathbf{n}_{1,2}\cdot\mathbf{k}$. With $H_{\mathcal{C}}$ and $H_{\mathcal{C}'}$, we can derive the phase shift after averaging over sky directions of the GWs and their initial phases. For example, considering the longitudinal mode, we have

$$H'_{\mathcal{C}}-H_{\mathcal{C}}=\frac{\pi h_l}{\omega_g\lambda_e}\left\{(\sin[\omega_g L_1(1-\mathbf{n_1}\cdot\mathbf{k})+\psi]-\sin\psi)\left(\frac{1}{1-\mathbf{n_1}\cdot\mathbf{k}}-\frac{1}{1-\mathbf{n_2}\cdot\mathbf{k}}\right)+(\sin[\omega_g L(1-\mathbf{k}\cdot\mathbf{n}+\psi]-\sin\psi)\left(\frac{1}{1-\mathbf{n_2}\cdot\mathbf{k}}-\frac{1}{1-\mathbf{k}\cdot\mathbf{n}}\right)\right\}. \tag{5}$$

The expression of $(H'_{\mathcal{C}}-H_{\mathcal{C}})^2$ follows obviously from Eq. (5). After averaging over the random initial phase ψ, and then performing an average over the azimuthal angle around n direction, we arrive at

$$(H'_{\mathcal{C}}-H_{\mathcal{C}})^2\approx\frac{\pi^2 h_l^2\alpha^2(2-\xi)}{2\omega_g^2\lambda_e^2\xi^3}\left\{(1-\cos[\omega L_1\xi])\frac{1}{1+r}-(1-\cos[\omega L\xi])\frac{r}{(1+r)^2}+(1-\cos[\omega L_2\xi])\frac{r}{1+r}\right\}. \tag{6}$$

At last the above expression is averaged for ξ (from 0 to 2) and that gives the corresponding $\delta\Phi^2$ or

$$\delta\Phi=\frac{\pi h_l\alpha L}{\lambda_e}\sqrt{\frac{r}{2(1+r)}}\sqrt{\log(1+r)+r\log\frac{1+r}{r}}. \tag{7}$$

In fact, for other polarizations, we can follow a similar procedure to compute the transfer functions. Their scalings are

$$\delta\Phi^2\equiv\langle(H_{\mathcal{C}}-H_{\mathcal{C}'})^2\rangle\propto\frac{h_m^2\alpha^2}{\omega_g^2\lambda_e^2}\times\begin{cases}\log(\omega_g L), & A=+,\times b,\\ \omega_g L, & A=x,y,\\ \omega_g^2 L^2, & A=l,\end{cases} \tag{8}$$

assuming $\omega_g L\gg 1$ (in the mHz band it is greater than 10^8 for typical pulsars). In particular, we find that the longitudinal mode ("l") receives the largest amplification factor

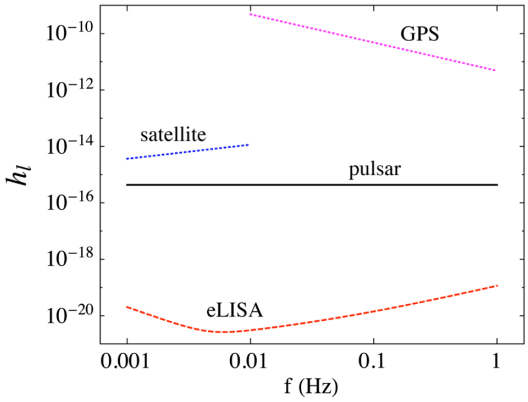

FIG. 2. The constraint on the dimensionless amplitude of longitudinal scalar GWs. The lines correspond to sensitivity curves given by previous Doppler tracking of spacecraft [13,14] (blue dotted), GPS satellites [15] (magenta dotted), pulsar scintillation from PSR B0834 + 06 ($r \sim 0.64$, $\alpha \sim 20$ mas/$r \sim 31$ mas, and $L \sim 640$ pc [2,12], black solid), and future eLISA measurements (red dashed), respectively. Notice that with the triangular geometry of eLISA, it is difficult to separate out different polarizations of GWs.

($\propto \omega_g^2 L^2$), while the amplitudes of all other polarizations are suppressed due to the transverse nature of GW propagation. For this reason, here we focus on the longitudinal mode.

Combining the longitudinal transfer function with the timing noise estimate given in the previous section, we can obtain the sensitivity of pulsar scintillation measurements of longitudinal scalar GWs, by making $\delta\Phi = 2\pi c \delta t_{\rm f}/\lambda_e$. Taking $r \sim 1$, this gives the sensitivity of h_l (dimensionless GW amplitude) as

$$h_l = 6.8 \times 10^{-18} \frac{\delta t_{\rm mHz}}{1\ {\rm ps}} \left(\frac{\alpha}{\rm arcsec}\right)^{-1} \left(\frac{L}{\rm kpc}\right)^{-1}. \quad (9)$$

In Fig. 2, we compare the sensitivity to longitudinal scalar GWs based on scintillation measurements of PSR B0834 + 06 (from Refs. [7,12]) with the current best constraint from Doppler tracking of the Cassini spacecraft in Refs. [13,14] and timing measurements of the GPS system in Ref. [15] and the proposed sensitivity of eLISA in the same frequency band. As discussed earlier, the SNR of scintillation measurements varies for different opening angles, and in practice the optimal opening angle could be different from the 25 mas limit obtained in Ref. [12]. These sensitivities are computed by considering the transfer functions of the scalar longitudinal mode, which give approximately the same responses as the tensor mode for Doppler timings and eLISA below 0.1 Hz [16] but better sensitivity than eLISA above 0.1 Hz. We can see that scintillation measurements from PSR B0834 + 06 already improve the previous sensitivity by a factor of 10–10^6 (a greater improvement compared to the GPS limit). By choosing more distant pulsars, larger opening angles, and/or the ones with better scintillation timing accuracy, as well as statistically averaging data for different scintillating pulsars, it is possible to dramatically improve this limit.

III. CONSTRAINT ON THE SCALAR-TENSOR RATIO OF GWs

It would be convenient to define the ratio of the GW amplitude in the scalar mode to that in the tensor mode as $R_{\rm ST} \equiv h^S/h^T$ and useful to show the upper limit in terms of $R_{\rm ST}$. The advantage of using $R_{\rm ST}$ is that it can be interpreted as the relative strength of the scalar coupling in a gravity theory to that of the ordinary gravitational (tensor) coupling, because the ratio is irrespective of common factors between the scalar and tensor modes, e.g. distance to the source and the direction of propagation in the interstellar space. It should be emphasized that in general in modified gravity theory, the scalar coupling strength depends on an environment in the Universe, the so-called screening mechanism, e.g. the chameleon mechanism, the Vainshtein mechanism, etc. [17,18]. Our constraint is obtained in a low-density and weak-gravity region (in a cosmological sense). In a high-density and stronger-gravity region such as near a GW source or on the Earth, a relatively large deviation from general relativity is allowed where the screening mechanism is also likely to operate. However, that part of the contribution is highly model dependent.

To derive the upper limit on $R_{\rm ST}$, what we need is the upper limit on the scalar amplitude in Eq. (9) and the amplitude in the tensor mode. The latter is source dependent and has a large uncertainty, depending on astrophysical scenarios. Thus we take into account this uncertainty, adopting the lowest, intermediate, and highest event rates among predictions in the literature when we derive the power spectrum densities S_h of each GW source. For white dwarf (WD) binaries, the extragalactic component dominates at $f > 1$ mHz and the spectrum has been estimated in Ref. [19] as $S_h^{\rm WD}(f) = \{0.37, 1.4, 2.3\} \times 10^{-46} (f/{\rm Hz})^{-7/3} \times \exp[-f/0.01\,{\rm Hz}]\,{\rm Hz}^{-1}$, with each corresponding to the lowest, intermediate, and highest event rates. For neutron star (NS) binaries, compiling the present merger rate [20] and its redshift evolution [21] gives $S_h^{\rm NS}(f) = \{0.016, 1.6, 16\} \times 10^{-47} (f/1\ {\rm Hz})^{-7/3}$ below the kHz band. For black hole (BH) binaries, the recent detection of a massive BH binary indicates that the merger rate of BH binaries may be higher than previous expectations [22]. Although the power spectrum of the GWB depends on models of BH binary formation, the *fiducial* model in Ref. [22] gives $S_h^{\rm BH}(f) = \{0.86, 4.7, 16\} \times 10^{-47} (f/1\ {\rm Hz})^{-7/3}$ without a high-frequency cutoff in the frequency band of our interest.

In Fig. 3, the constraints on $R_{\rm ST}$ for each GW source are shown. The upper bounds are tighter at lower frequencies,

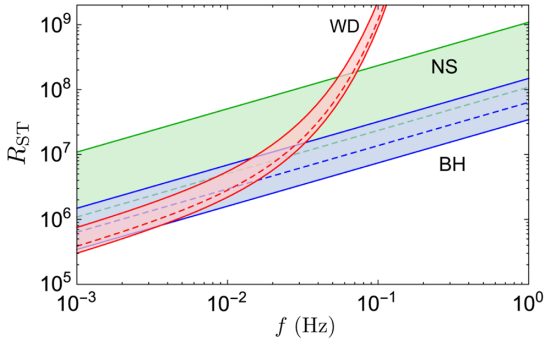

FIG. 3. Upper limit on the scalar-to-tensor ratio R_{ST} for each GWB source with uncertainties of merger rates: WD binaries (red), NS binaries (green), and BH binaries (blue). The dashed lines correspond to the intermediate merger rates and the solid lines are the lowest and highest merger rates.

which at 1 mHz are 3.9×10^5, 1.1×10^6, and 6.4×10^5 for the intermediate merger rates of WD, NS, and BH binaries, respectively. Although the numerical values appear to be much larger than one, they are the first constraints on R_{ST} obtained in the frequency band from 1 mHz to 1 Hz in the low-density and weak-gravity region of space, and they connect the physics of GW emission of a source and a screening mechanism in a model-independent way. There have been constraints at different frequencies from other observations. The observation of the orbital-period derivative from PSR B1913 + 16 agrees well with predicted values of GR, conservatively, at a level of 1% error [23]. This fact indicates that the contribution of scalar GWs to the energy loss is less than 1%, that is, $R_{ST} \lesssim 10^{-1}$ at 7.2×10^{-5} Hz at the source position of the NS binary. On the other hand, the recent detection of GWs (GW150914) [24] gives no constraint on the scalar component, as at least three detectors are needed to break the degeneracy of the polarization modes [25].

IV. DISCUSSION AND CONCLUSION

Compared to single-path pulsar timing measurements, the scintillation measurements have better timing accuracies, and phase-comparison geometry which naturally removes intrinsic noise from the source. These are the key factors that ensure its ultra precision and enable its application to studying ISM physics, pulsar physics, and our proposal in this paper: testing alternative gravity models.

We have illustrated an example in this proposal: measuring a longitudinal scalar GWB. It is also possible to apply it to other tests which do not involve GWs; for example, spacetime quantum fluctuations [26,27] or holographic noise [28]. They would contribute distinctive phase noise for photons traveling along different scintillation paths, and hence can be measured by observing the anomalous scintillation phase shift or a degrading of the interference pattern.

ACKNOWLEDGMENTS

The authors appreciate many helpful comments from the referees, especially regarding many aspects of the scintillation discussions. H. Y. thanks I-Sheng Yang for very instructive discussions on the timing noise of pulsar scintillations and Nestor Ortiz for making Fig. 1. H. Y. acknowledges support from the Perimeter Institute of Theoretical Physics and the Institute for Quantum Computing. A. N. is supported by NSF CAREER Grant No. PHY-1055103 and the H2020-MSCA-RISE-2015 Grant No. StronGrHEP-690904. A. N. thanks the hospitality of Perimeter Institute, where part of the work was performed. Research at Perimeter Institute is supported by the government of Canada through the Department of Innovation, Science and Economic Development Canada and by the Province of Ontario through the Ministry of Research and Innovation.

[1] U.-L. Pen and Y. Levin, Mon. Not. R. Astron. Soc. **442**, 3338 (2014).
[2] S. Liu, U.-L. Pen, J.-P. Macquart, W. Brisken, and A. Deller, Mon. Not. R. Astron. Soc. **458**, 1289 (2016).
[3] U.-L. Pen, J.-P. Macquart, A. T. Deller, and W. Brisken, Mon. Not. R. Astron. Soc. **440**, L36 (2014).
[4] B. J. Rickett, Annu. Rev. Astron. Astrophys. **15**, 479 (1977).
[5] B. J. Rickett, Astrophys. J. **307**, 564 (1986).
[6] M. D. Johnson, C. R. Gwinn, and P. Demorest, Astrophys. J. **758**, 8 (2012).
[7] M. A. Walker, L. V. E. Koopmans, D. R. Stinebring, and W. van Straten, Mon. Not. R. Astron. Soc. **388**, 1214 (2008).
[8] D. M. Eardley, D. L. Lee, A. P. Lightman, R. V. Wagoner, and C. M. Will, Phys. Rev. Lett. **30**, 884 (1973).
[9] A. Nishizawa, A. Taruya, K. Hayama, S. Kawamura, and M. Sakagami, Phys. Rev. D **79**, 082002 (2009).
[10] K. J. Lee, Classical Quantum Gravity **30**, 224016 (2013).
[11] P. Amaro-Seoane, S. Aoudia, S. Babak, P. Bintruy, E. Berti, A. Boh, C. Caprini, M. Colpi, N. J. Cor- nish, K. Danzmann *et al.*, Classical Quantum Gravity **29**, 124016 (2012).
[12] W. F. Brisken, J.-P. Macquart, J.-J. Gao, B. Rickett, W. Coles, A. Deller, S. Tingay, and C. West, Astrophys. J. **708**, 232 (2010).
[13] B. Bertotti *et al.*, Astron. Astrophys. **296**, 13 (1995).

[14] J. W. Armstrong, L. Iess, P. Tortora, and B. Bertotti, Astrophys. J. **599**, 806 (2003).
[15] S. Aoyama, R. Tazai, and K. Ichiki, Phys. Rev. D **89**, 067101 (2014).
[16] M. Tinto and M. E. da Silva Alves, Phys. Rev. D **82**, 122003 (2010).
[17] J. Khoury and A. Weltman, Phys. Rev. D **69**, 044026 (2004).
[18] A. I. Vainshtein, Phys. Lett. B **39**, 393 (1972).
[19] A. J. Farmer and E. S. Phinney, Mon. Not. R. Astron. Soc. **346**, 1197 (2003).
[20] J. Abadie *et al.*, Classical Quantum Gravity **27**, 173001 (2010).
[21] C. Cutler and J. Harms, Phys. Rev. D **73**, 042001 (2006).
[22] LIGO Scientific and Virgo Collaborations, Phys. Rev. Lett. **116**, 131102 (2016).
[23] J. M. Weisberg, D. J. Nice, and J. H. Taylor, Astrophys. J. **722**, 1030 (2010).
[24] B. P. Abbott *et al.*, Phys. Rev. Lett. **116**, 061102 (2016).
[25] A. Nishizawa, A. Taruya, and S. Kawamura, Phys. Rev. D **81**, 104043 (2010).
[26] Y. J. Ng and H. van Dam, Mod. Phys. Lett. A **09**, 335 (1994).
[27] G. Amelino-Camelia, Nature (London) **398**, 216 (1999).
[28] C. J. Hogan, Phys. Rev. D **77**, 104031 (2008).